KSCE Journal of Civil Engineering (2021) 25(3):1008-1018
DOI 10.1007/s12205-020-1373-7

pISSN 1226-7988, eISSN 1976-3808
www.springer.com/12205

Structural Engineering

Assessment of Dynamic Response of 3D Ultra High Performance Concrete Frame Structure under High Explosion Using Johnson-Holmquist 2 Model

Viet-Chinh Mai[a] **and Ngoc-Quang Vu**[b]

[a]*Dept. of Civil Engineering, Kumoh National Institute of Technology, Gumi 39177, Korea*
[b]*Institute of Techniques for Special Engineering, Le Quy Don Technical University, Ha Noi 11355, Viet Nam*

ARTICLE HISTORY

Received 4 August 2020
Accepted 14 October 2020
Published Online 24 December 2020

KEYWORDS

Ultra High Performance Concrete
Blast loading
Tall building
Dynamic response
Damage
Johnson-Holmquist 2 model

ABSTRACT

Most of the 3D frame structures are not initially designed to resist blast loads. Due to the limitation of financial resources as well as the complex technical requirements, study the dynamic behavior of 3D frame structure under blast load, particularly for advanced materials like Ultra High Performance Concrete (UHPC), faces many challenges. Therefore, numerical simulation can be a good alternative. The objective of the research is to investigate the dynamic behavior of a UHPC building subjected to blast loading through a 3-D numerical model with the direct simulation of blast load. This building studied in this paper is a real, 6-story office building in Vietnam, which was originally designed for dead load, live load, wind, and earthquake. The building is subjected to surface blast of 500kg Trinitrotoluen (TNT) equivalent charge weight with close-in distance and a variable height of blast source. In this study, Johnson–Holmquist 2 damage model (JH-2) model is implemented to simulate the UHPC structures subjected to blast loading. Base on the theory of the JH-2 model, a subroutine, integrated with Abaqus software, is designed by the authors to calibrate the input parameters of UHPC material. A total of 8 cases of the explosion scenario are considered, in which the design of the original column is revised by using UHPC composite structure in external columns. The results indicate that there is a tremendous increase in response when the blast occurs at the mid-height of the building and the severe damage is observed in the external column in front of the explosion. The obtained result in terms of blast wave pressure during time history as well as peak deflections and damage of building under blast loading is assessed. The blast loading resistance effect of the revised design compared to the original design is also demonstrated as a beneficial alternative in blasting condition.

1. Introduction

According to the Global Terrorism Index report in 2019 (Institute for Economics & Peace, 2019), the global number of deaths from terrorism is down, however, the number of countries affected by terrorism is growing. A terror attack such as a bomb explosion in or near a building may have catastrophic effects, destroying or severely damaging portions of the exterior and interior structural framework of the building (Ngo et al., 2007). Therefore, the study to improve the protection of structures against the aforementioned extreme loading scenarios, particularly the building in crowded cities, is necessary. Conventional concrete including normal concrete and high strength concrete is a widely used material in structures of the society. This material also may be used in the design of structures to resist the explosion. There have been many studies on structures using conventional concrete under blast loading (Kong et al., 2018; Shin and Lee, 2018; Abbas et al., 2019; Shinde et al., 2019). The results indicated many advantages of conventional concrete like strength, durability, however, fragmentation, high deflection, strain rate, and energy absorption capacity are also disadvantages of this material (Buchan and Chen, 2010). Advancements in concrete material science led to the development of UHPC. Compared to conventional concrete, UHPC shows greater properties in

CORRESPONDENCE Viet-Chinh Mai maivietchinh@lqdtu.edu.vn Dept. of Civil Engineering, Kumoh National Institute of Technology, Gumi 39177, Korea

compressive strength, tensile resistance, and toughness (Wang et al., 2015; Yoo and Banthia, 2017; Azmee and Shafiq, 2018; Khairunnisa et al., 2018; Smarzewski, 2019; Tayeh et al., 2019). Moreover, due to including appropriate fiber ratio in the mix, UHPC has high ductility, great energy-dissipating capacity, and deformation capacity under dynamic load (Ousalem et al., 2009; Wang et al., 2016). These enhanced properties make UHPC an attractive material for use in the blast resistance design (Yoo and Banthia, 2017).

There have been some studies on buildings using conventional concrete under blast loading. Using a numerical model, Ibrahim and Nabi (2019) investigated the performance of 6-storey reinforced concrete building subjected to blast loading (Ibrahim and Nabil, 2019). The concrete damage plasticity model provided in ABAQUS was chosen to simulate the concrete elements. In general, this model is suitable to describe the constitutive law and behavior of brittle materials like concrete under cyclic and dynamic load. Concrete is cracked in tensile stress and crushed under compressive action are the main failure mechanisms of the Concrete Damaged Plasticity (CDP) model. When the pressure in the material reaches the confining value to limit the crack propagation, concrete no longer behaves as a brittle material. Hence, the CDP model designed in ABAQUS is just effective to describe the behavior of irreversible damage of material in low-pressure conditions (Dassault Systèmes Simulia Corp., 2016). In other words, simulation of the behavior of concrete under high pressure such as an explosion in a very short period is not suitable for this model. A 4-story reinforced concrete building simulation subjected to blast loading has been carried out by Ismail et al. (2017). The material constitutive relationship was performed using ABAQUS combined with the CDP model and brittle cracking concrete model in order to assess the structural behavior (Ismail et al., 2017). The response of the 3D frame structure after the explosion, including deformation, stress, and damage value were presented. Furthermore, based on obtained results, the revised cross-section by concrete-filled steel tube of external columns revealed remarkable benefits to improve the capacity of the structure in the blast loading condition. This design viewpoint of Ismail et al. is different from the design of the authors in the article, where the revised cross-section of external columns are covered with UHPC (UHPC composite) and the steel core is located in the center of the column to take advantage of the high strength in compression and tension of UHPC material. Draganic and Sigmund (2012) studied the effect of blast loading on the structure. They designed the process of evaluating the blast loading on structural components and a numerical example of a fictive structure was provided. By the numerical model in SAP2000, the blast loading was determined as a pressure-time history. A 7-story building subjected to blast load was analyzed to verify the above model (Draganić and Sigmund, 2012). However, simulation analysis in SAP might only describe the overall linear response of the structure under blast load and this method is not favorable to capture the nonlinear behavior of materials, especially the damage variable, which plays an important role in the explosive analysis. Weerheijm et al. (2009) investigated the dynamic response and progressive collapse of a multi-story reinforced concrete building. Based on the obtained results, they proposed the link between the loss of the building's functionality and its damaged state after the explosion (Weerheijm et al., 2009). Weerheijm et al. (2008) studied the damage of a reinforced concrete frame related to bombing incidents Weerheijm et al., 2008). It consists of two principal stages in the damage evaluation process. The first stage is the response of the structure under external blast loading and the next stage is to evaluate the residual capacities of the remaining structure after the explosion. Jayatilake et al. (2006) shed light on the structural behavior of a tall building subjected to blast loading. Three-dimensional nonlinear dynamic responses of the typical tall building as well as acceleration, maximum deflection, story drift, and bending moments at critical regions, were investigated (Jayatilake et al., 2006).

Despite the fact that experimental tests play an important role in shedding light on the dynamic behavior of structures under blast loading, however, these experiments are hugely costly and require complicated technical systems, particularly for full-scale structures like multi-story buildings. Hence, the finite element method is much needed to provide related supplementary knowledge on quantifying and predicting explosion damage of framed building subjected to blast effect and become the main approach for the related research. This study developed an extensive finite element model to investigate the dynamic response of the UHPC frame structure subjected to blast loading and contributes to its application of UHPC in the new material technology field for designing structures to resist blast load.

2. Material Model and 3D Simulation Model

Due to the sensitive structural response of concrete material, for the numerical analysis, choosing a suitable material model is important. In general, concrete material exhibits the ductile property under hydrostatic pressure (Cui et al., 2017) and experiences brittle failure in tension conditions. There are available several material models in the LS DYNA software library for modeling concrete material under blast loading (Livermore Software Technology Corporation, 2003). Based on Eurocode-2, MAT_CONCRETE_EC2 (also known as *MAT_172), which can be applicable to quasi-static, basic structural applications and cyclic loading e.g., seismic. Nevertheless, it is not suitable for high strain-rate applications. It uses a smeared combination of concrete and steel to simulate reinforced concrete. This approach is efficient in order to model large structures such as tall buildings. Mat Concrete Dam- Age-Rel3 (MAT_72R3) material model is suitable to simulate the behavior of concrete material under extreme dynamic loadings. Some researchers indicated that MAT_72R3 model can successfully incorporate non-linear concrete properties (Bao and Li, 2010; Thilakarathna et al., 2010). Unconfined compressive strength is a user input parameter, which can be obtained by experiments, is sufficient to implement the numerical model. This is another advantage of this model.

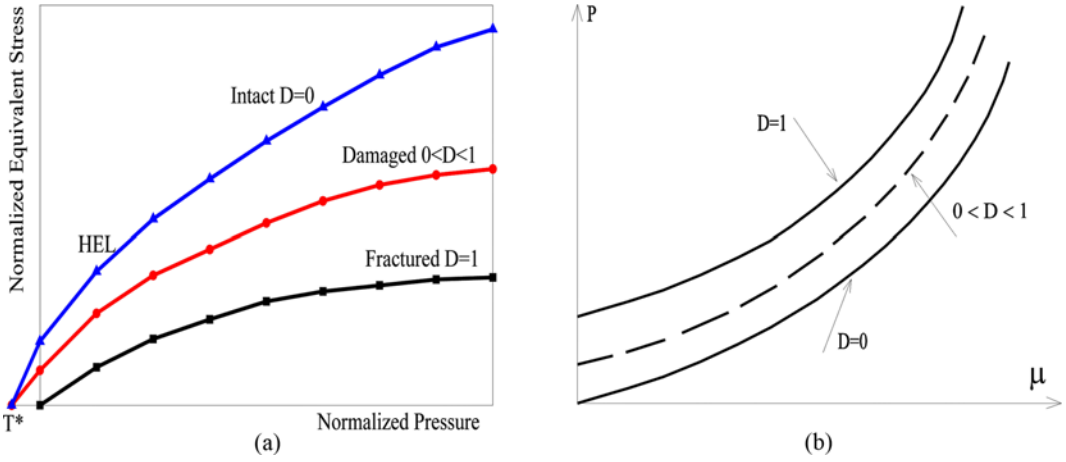

Fig. 1. Description of the Johnson–Holmquist 2 Model: (a) Strength, (b) Pressure P and Volumetric Strain μ

However, as mentioned above, UHPC is an advanced concrete and the difference in UHPC mix compared to conventional concrete leads to its unique characteristics. Designing and applying more sophisticated model that can accurately capture the behavior of UHPC under blast load is very necessary.

Johnson–Holmquist damage model is used to model the mechanical behavior of brittle materials over a range of strain rates, which have high compressive strength but low tensile strength and tend to experience progressive damage under dynamic load due to the growth of microfractures. The Johnson–Holmquist (JH-1) (Johnson and Holmquist, 1992) model is the original version that was developed to account for large deformations but did not take into consideration progressive damage with increasing deformation. The Johnson-Holmquist 2 model (JH-2) is the second version of the JH-1 (Holmquist et al., 1993). Fig. 1 shows the description of the Johnson–Holmquist 2 model.

In JH-2 model, the relationship between normalized intact equivalent stress and damage state can be expressed as

$$\sigma^* = \sigma_i^* - D(\sigma_i^* - \sigma_f^*), \tag{1}$$

where σ_i^*, σ_f^* represent the normalized intact equivalent stress and the fracture strength, respectively;

$0 \le D \le 1$ denotes the scalar damage parameter.

After normalization, stress in Eq. (1) can be rewritten as

$$\sigma^* = \sigma / \sigma_{HEL}, \tag{2}$$

where σ_{HEL} presents the Hugoniot Elastic Limit (HEL) pressure state σ_i^*, σ_f^* can be obtained through

$$\sigma_i^* = A(P^* + T^*)^N / (1 + C \ln \dot{\varepsilon}^*), \tag{3}$$

$$\sigma_f^* = B(P^*)^M (1 + C \ln \dot{\varepsilon}^*), \tag{4}$$

where the material constants are A, B, C, M, and N. $\dot{\varepsilon}^*$ is the strain rate.

P^* is the normalized pressure and T^* represents the normalized maximum tensile hydrostatic pressure.

All damage D is accumulated by incremental plastic deformation $\Delta\varepsilon_f^p$ in the equation

$$D = \sum \Delta\varepsilon^p / \varepsilon_f^p, \tag{5}$$

where $\Delta\varepsilon_f^p$ is the deformation of incremental plastic.

ε_f^p represents the independent plastic strain, is given as

$$\varepsilon_f^p = D_1 (P^* + T^*)^{D_2}. \tag{6}$$

D_1 and D_2 are material constants.

The hydrostatic pressure P can be given through

$$P = K_1 \mu + K_2 \mu^2 + K_3 \mu^3 + \Delta P, \tag{7}$$

where K_1, K_2, K_3 are the material parameters; DP is an additional pressure increment after damage begins. $\mu = \rho/\rho_0 - 1$ is the volumetric strain; ρ and ρ_0 represent the final and initial density, respectively.

Based on the theory of the JH-2 model, the authors designed a subroutine with FORTRAN language, including 32 mechanical constants and 8 numbers of solution-dependent state variables. These state variables consist of Equivalent plastic strain (FEEQ), Ductile damage initiation criterion (DUCTCRT), Pressure increment due to bulking (DELTAP), or Damage (D), etc. Using User-defined mechanical material behavior in ABAQUS, whereby any mechanical constitutive model can be added to the library. The feature requires a constitutive model in the user's subroutine such as VUMAT (ABAQUS /Explicit) with considerable effort and expertise. Fig. 2 describes the subroutine and Global Flow in ABAQUS, where User Subroutines Fit into ABAQUS (Dassault Systèmes Simulia Corp., 2016). In these figures, a ▭ represents a specific state or a decision point in the code (i.e., beginning of increment) during the analysis. A ▭ indicates an action that is taken during the analysis. K^{el} is the material matrix. R^a represents the external force vector and C is the displacement vector of the model. Before the step of increment determination, the model is performed as a common analysis in ABAQUS. At the step of defining material, based on the JH-2 model, the properties of the UHPC are defined through a subroutine which is inserted into the ABAQUS software. The input parameters of the JH-2 model

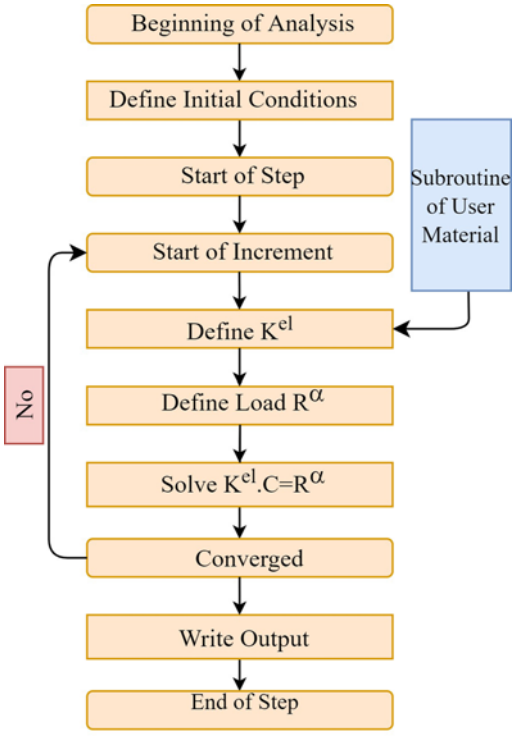

Fig. 2. Flow Chart of the Subroutine for the Proposed Model

for UHPC material and material parameters for steel bar SD400 are presented in Tables 1 and 2, respectively.

The structure selected for this study is a 6-story building, having a plan dimension of 28.8 × 10.8 m. The height is 3.6 m for each story and the slab's thickness is 130 mm. Grade S400 steel is used for the reinforcement bar. The typical beam size is 600 × 400 mm, column size is 600 × 600 mm. The structural layout is illustrated in Fig. 3. According to TCCN2737-1995 (Vietnamese Ministry of Construction, 2011) live load value is applied to the slabs at the level of each floor and wall load is applied as a uniformly load on the beams. The original building is designed to resist the earthquake. The building is classified as a category II construction with an importance factor of 1.0 in the Vietnamese earthquake code (Vietnamese Ministry of Construction, 2013). Explosions include the external and internal explosion, which can be a package bomb, vehicle bomb, or incendiary devices (Fu, 2013). Compared to other attack types, package bombs are much more difficult to prevent (Yandzio, 1999). So, in this article, the package bomb was selected. Base on the obtained results, Ambrosini et al. concluded that 200 – 500 kg TNT equivalent of package bomb attack might cause damage to buildings the same to a medium terrorist attack (Ambrosini et al., 2005). Another study demonstrated that a 1ton of TNT equivalent with a 5 m stand-off distance from the structure for an external explosion is reasonable (Dept. of Defense, 2008). Therefore, charge weight of 500 kg of TNT equivalent is suitable for the medium-sized building with six stories. For each of these cases, the height of the charge weight from the ground is 1 m and 10 m, respectively. On the other hand, in order to investigate the dynamic behavior of the building under blast loading, stand-off distance is varied from 5 m and 10 m. Normally, the structural components directly exposed to the blast source are most vulnerable. Hence, to improve the blast resistant design for frame structure, the external columns facing the blast load should be carefully considered. According to this premise, the models with and without monolithic steel column sections are created. For each scenario, the obtained results after

Table 1. The Material Parameters of the JH-2 Model for UHPC

Variable	Description	Value
ρ (Ton/mm^3)	Density	2.55e^{-9}
f_c (MPa)	Compressive strength	140
E (MPa)	Young's Modulus	44617
ν	Possion's ratio	0.2
G (MPa)	Shear Modulus	26770
A	The material constant	1.41
B	The material constant	0.79
C	The material constant	0.118
N	The material constant	0.77
$\dot{\varepsilon}_0$	The reference strain rate	1
D_1	Damage parameter	0.073
D_2	Damage parameter	1
σ_{HEL} (MPa)	The equivalent stress at the Hugoniot	510
P_{HEL} (MPa)	The hydrostatic pressure	250
μ_{HEL}	Volumetric strain at HEL	0.0834
K_1 (GPa)	The material parameter of State Constant	22.7
K_2 (MPa)	The material parameter of State Constant	17.1
K_3 (MPa)	The material parameter of State Constant	20.8

Table 2. The Material Parameters for Steel Bar SD400

Variable	SD400
Elastic Modulus (MPa)	205940
Poission's Ratio	0.3
Weight density (N/mm^3)	7.7e^{-5}
Yeild strength (MPa)	400
Ultimate strength (MPa)	560

Table 3. Blast Loading Scenarios

Case	TNT equivalent	Distance from the ground (H)	Distance from the building (Z) volume (%)	The external columns
1	500 kg	1 m	5 m	UHPC
2	500 kg	1 m	5 m	UHPC composite column
3	500 kg	1 m	10 m	UHPC
4	500 kg	1 m	10 m	UHPC composite column
5	500 kg	10 m	5 m	UHPC
6	500 kg	10 m	5 m	UHPC composite column
7	500 kg	10 m	10 m	UHPC
8	500 kg	10 m	10 m	UHPC composite column

the blast analysis of the original structural design are compared with a revised design, which uses the UHPC composite cross-sections for all external columns. The revised UHPC cross-section is shown in Fig. 3. Blast loading scenarios are listed in Table 3.

3. Results and Discussion

3.1 Verification of the Proposed Model

It is necessary to validate the proposed model to verify the accuracy of the modeling and corresponding results. The important aspects to be verified are the constitutive model used in the non-linear investigation and structural response. Based on the theory of JH-2 model, a study was implemented by the authors in which three UHPC panels with different steel bar volume and stand-off distances of charge point were analyzed. The simulation results were compared against the experimental results of Mao (Mao et al., 2014). A close agreement between the tests and simulation results was obtained and presented in the

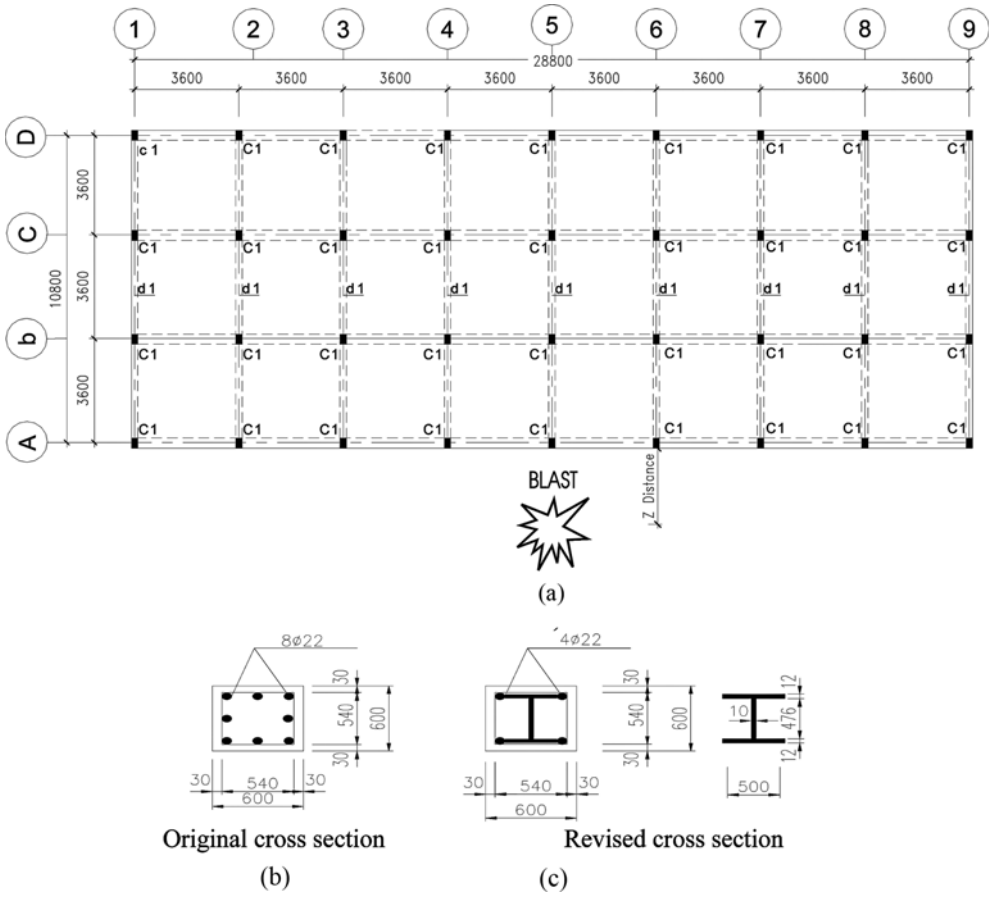

Fig. 3. Base Layout of the Building: (a) Typical Structural Floor Plan, (b) Original Cross-section, (c) Revised Cross-section of the Column

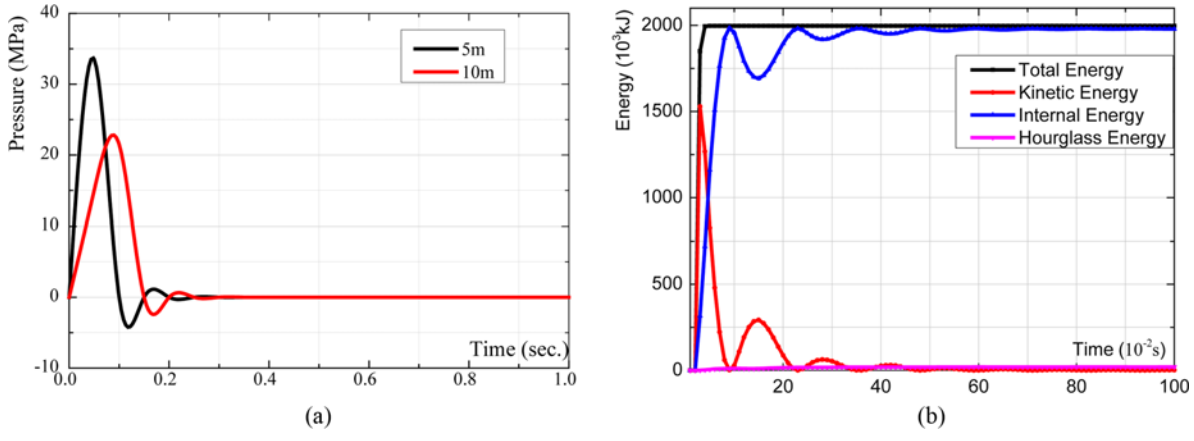

Fig. 4. Blast Simulation Result: (a) Blast Wave Pressure with Various Stand-Off Distances, (b) Energy of Blast

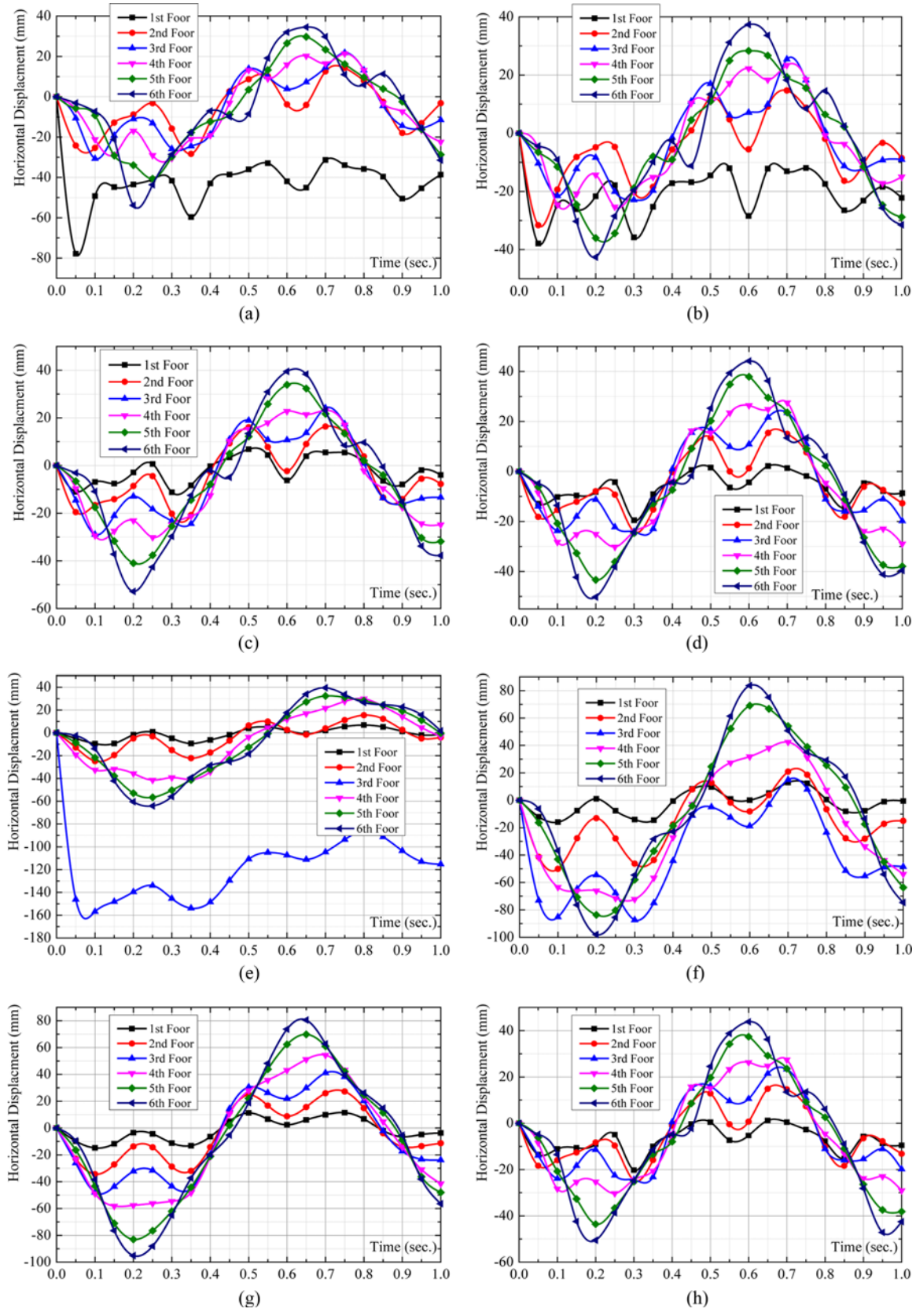

Fig. 5. Maximum Mid-span Deflection and Permanent Deflection of the UHPC Columns: (a) H = 1 m; Z = 5 m (without composite columns), (b) H = 1 m; Z = 5 m (composite columns), (c) H = 1 m; Z = 10 m (without composite columns), (d) H = 1 m; Z = 10 m (composite columns), (e) H = 10 m; Z = 5 m (without composite columns), (f) H = 10 m; Z = 5 m (composite columns), (g) H = 10 m; Z = 10 m (without composite columns), (h) H = 10 m; Z = 10 m (composite columns)

article of Mai et al. (Mai et al., 2020).

3.2 Pressure and Energy Results

Blast wave pressure and energy results after the explosion are presented in Fig. 4. The peak of blast overpressure, P_{so}, for 500 kg TNT equivalent with 5 m and 10 m distance from the building are 33.2 and 23.8 MPa, respectively. Hourglass energy represents the artificial strain energy of the whole model. The smaller this value is, the more accurate the numerical simulation result can be obtained. Hallquist et al. revealed that for blast simulation, the hourglass energy should not be higher than 10% value of the internal energy (Hallquist et al., 1995). In Fig. 4, the maximum hourglass energy is nearly 25.10^3kJ, which accounts for 1.25% in internal energy (2,000. 10^3kJ). This result verified the accuracy of the simulation model.

3.3 Deflection Result

To facilitate the following discussion, study cases with different stand-off distance, the height of detonation, and the revised design of column cross-sections are listed in Table 2. Cases 1, 3, 5, 7 imply that the building does not have UHPC composite columns which are analyzed in various blast loading conditions. In contrast, cases 2, 4, 6, 8 refer to the structure designed by UHPC composite columns. Horizontal displacement and damage variables are the two important factors to determine the structural behavior. According to Fig. 5 and Table 4, the parametric study proves that decreasing the stand-off distance Z and increasing height H from the ground of the explosion leads to a significant increment in horizontal displacement. The increase of horizontal displacement does not depend on the type of structure (with or without UHPC composite columns). For instance, for cases 1 and 3, when the distance Z decreases from 10 m to 5 m, the maximum displacement increases nearly 1.5 times (from 51.5 mm to 79.1 mm). For cases 2 and 6, following the increase of height H from 1 m to 10 m, the peak displacement increases 2.3 times (from 42.3 mm to 98.8 mm). Apparently, the horizontal displacement attains the maximum value when the blast occurs at the mid-height of the building.

For the 10m distance along the Z direction, due to enough high stand-off distance, the natural period of the building is the same as the loading duration of the blast. Therefore, pressure and impulse doesn't have a significant effect on the dynamic behavior of the structure. However, for the 5 m stand-off distance, blast wave duration is smaller than the natural period of the building. Consequently, the impulsive control region is formed resulting in a remarkable effect increment on the structural behavior of the building. Unlike the behavior of the structure under earthquake and wind, the building subjected to blast load doesn't show the response as a cantilever structure, where displacement variation is non-uniform through the height of the building.

Other important knowledge can be obtained from simulation results. Under the same conditions of the explosion, distance (Z), height (H), etc., the building with UHPC composite cross-sections (cases 2, 4, 6, 8) for all external columns show remarkably smaller displacement than building without UHPC composite column (cases 1, 3, 5, 7). For instance, the model without UHPC composite columns (case 5) shows a displacement of 161.4 mm, which is 1.6 times higher compared to the 98.8 mm of the model with UHPC composite columns (case 6). Case 7 (without UHPC composite columns) in comparison to case 8 (with UHPC composite columns) presents the 1.8 times higher value of displacement (96.2 mm and 52.6 mm). Moreover, using UHPC composite columns causes a change in the behavior of the structure. In the cases of the building without UHPC composite columns (cases 1, 3) the maximum horizontal displacement can be observed on the first floor and the third floor that is close to the explosion. In view of the aforementioned explanation, the main cause is the impulse impact of blast loading. In contrast, the building with external UHPC composite columns (cases 2, 6) not only shows the remarkably smaller peak displacement but also changes in the region of maximum displacement. For these cases, the maximum horizontal displacement can be seen on the 6th floor, instead of the 1st and 3rd floors as in cases 1 and 5. This demonstrates that using composite columns lead to re-distribution on the impact of the impulse in the structure and minimize significantly its impact on the building. Although there is not enough data to compare the peak horizontal displacement and residual displacement of this building under blast loading to the seismic load, however, the assessment of damage level for this building in the next section will also provide more knowledge about the dynamic response of the building under blast loading compared to the seismic loading.

Table 4. Maximum Horizontal Deflection of the Building

Case	Location	The external columns	Value of deflection (mm)
1-a	1st floor	UHPC	79.1
2-b	6th floor	UHPC composite column	42.3
3-c	6rd floor	UHPC	51.5
4-d	6th floor	UHPC composite column	50.8
5-e	3rd floor	UHPC	161.4
6-*f*	6th floor	UHPC composite column	98.8
7-g	6th floor	UHPC	96.2
8-h	6th floor	UHPC composite column	52.6

3.4 Damage Result

The damage profile of the building after the explosion is shown in Fig. 6, Tables 5 and 6. Figs. 6(a), 6(c), 6(e), 6(g) describe the damage state of the building under blast loading condition of cases 1, 3, 5, 7 in which the 3D frame structure has the original design. Figs. 6(b), 6(d), 6(f), 6(h) show the damage state when the building is applied revised design in all external columns, corresponding to cases 2, 4, 6, 8.

Basically, the damage state of all structural elements tends to be similar to horizontal displacement, which means increasing vertical (H) distance and decreasing horizontal (Z) distance of charge point leads to considerable increment in the amount of

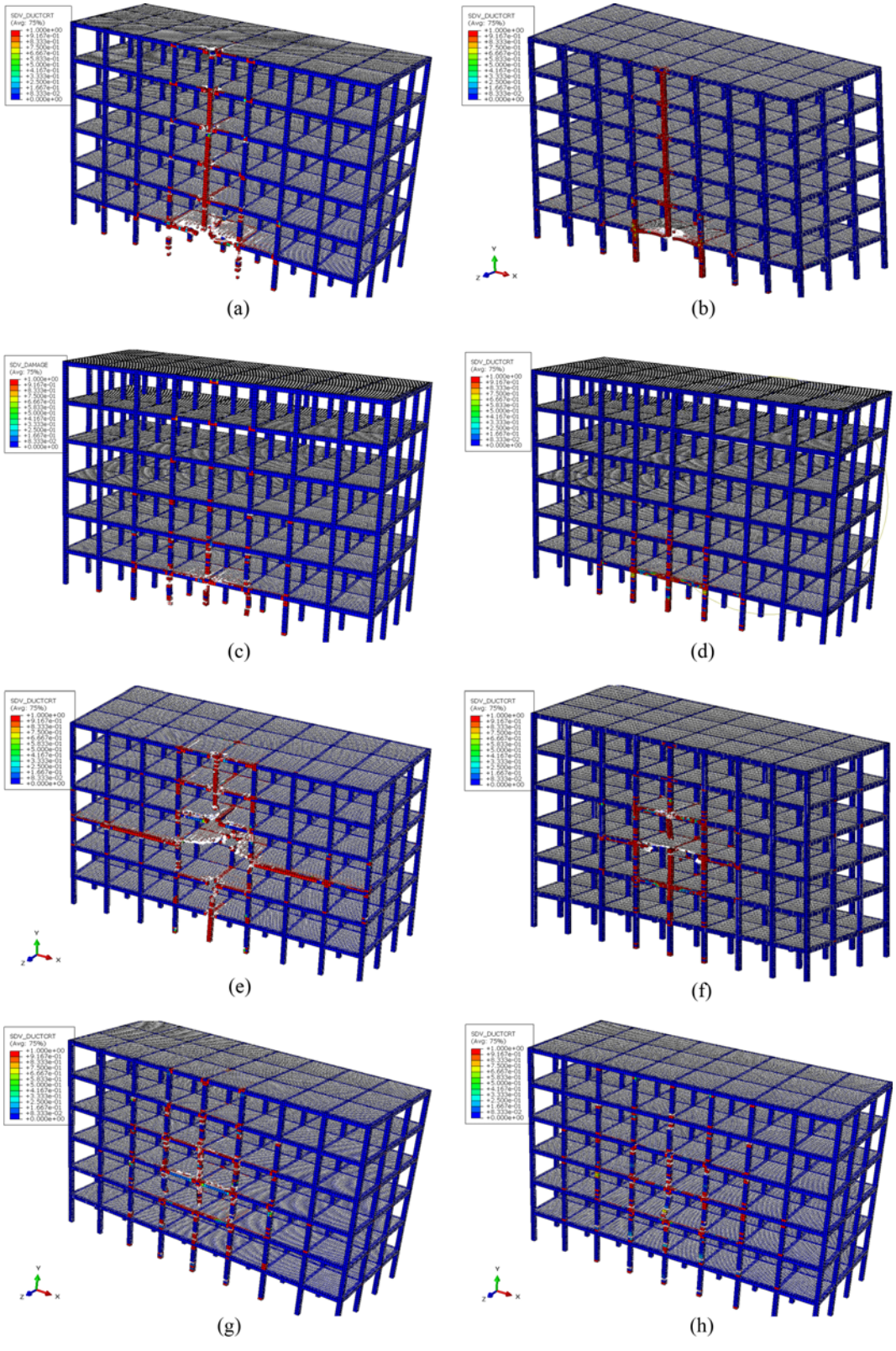

Fig. 6. Damage Profile of the Building after the Explosion: (a) H = 1 m; Z = 5 m (without composite columns), (b) H = 1 m; Z = 5 m (composite columns), (c) H = 1 m; Z = 10 m (without composite columns), (d) H = 1 m; Z = 10 m (composite columns), (e) H = 10 m; Z = 5 m (without composite columns), (f) H = 10 m; Z = 5 m (composite columns), (g) H = 10 m; Z = 10 m (without composite columns), (h) H = 10 m; Z = 10 m (composite columns) (Case 1: a, Case 2: b, Case 3: c, Case 4: d, Case 5: e, Case 6: f, Case 7: g, Case 8: h)

Table 5. Summary the Structural Elements of the Building

Column (Quantity)	Beam (Quantity)	Slab (m^2)
36	144	1866.24

Table 6. Serve Damage State of the Building after the Explosion

Case	The external columns	Column (%)	Beam (%)	Slab (%)
1-a	UHPC	33.3	13.2	4.16
2-b	UHPC composite column	19.4	4.1	2.0
3-c	UHPC	13.8	2.8	1.4
4-d	UHPC composite column	2.7	0	0.1
5-e	UHPC	38.8	16.7	5.4
6-f	UHPC composite column	25	6.2	2.7
7-g	UHPC	19.4	3.5	1.6
8-h	UHPC composite column	22.2	4.9	2.1

damage in the structure. For example, with the original design, as the stand-off distance Z decreases from 10 m (case 3) to 5 m (case 1), the severe damage in columns, beams, floors increases from 13.8% to 33.3%, 2.8% to 13.2%, and 1.4% to 4.16%, respectively. For all calculated cases, the external column exposed to the explosion experiences the most damage, yet the damage of columns inside the building (away from the explosion) is remarkably small than the rest. After the first step of blast loading impact at 0.1s, the building is deformed progressively, plastic hinges are formed at the column-beam intersection and the frame structure tends to be collapsed partially around this position. Excessive damage also occurs to two slabs of spans behind these external columns.

It is well known that the column elements are very important to prevent the collapse of frame structure subjected to blast loading. Therefore, the discussion of the obtained results focuses mainly on the dynamic response and damage state of the columns under the explosive load. Careful observation of results the Fig. 6 and Table 6 demonstrates that the building with the original design (without composite columns) is severely damaged under the explosion than the building with the revised design (UHPC composite columns). For instance, with the same blast loading condition, the severe damage of the columns (38.8%) in case 5 (original design), is 1.5 times greater than the revised design (25%) in case 6. It can be seen that changing the design of the various input parameters, including material, cross-section, etc., especially for elements adjacent to the blast loading can strengthen significantly the overall performance of the structure.

Let us now investigate the effect of the revised design on the damage propagation of the building under blast load. For case 1 (without UHPC composite columns), progressive collapse occurs to the external frame of the building exposed to the explosion source. The local collapse near the ground level causes severe damage up to the upper floor at the front side of the building. On the contrary, for case 2 (with UHPC composite columns), plastic hinges are limited to the external frame of building exposed to blast loading. Severe damage just occurs to a few columns and beams. For case 5 (without UHPC composite columns), when the explosion is placed at mid-height of the frame structure, there is a tremendous increase in the damage state of structural elements. Compared to the case of 1 m height explosion, severe damage and a remarkable amount of plastic hinges are formed in the frame exposed to blast loading, which extends to adjacent columns and beams, as well as to most of the beam-column intersections. This is because in the front of the building covering much more area of the structure exposed to blast loading. The columns and beam-column intersections under severe blast loading condition leading to the formation of plastic hinges, and these columns lost loading capacity, subsequently resulting in the progressive collapse of the structure. Due to blast wave, the external columns are suddenly removed resulting in the redistribution of the load carried by the frame structure, implying the increment in internal force of other remained columns. For cases 1, 3, 5, and 7, not only the external frame exposed to blast loading but also the structures in the second rows of columns are rather damaged. Compared to the case without UHPC composite columns, external columns are reinforced with UHPC composite section in cases 2, 4, 6, 8 shows only some damage on the face next to the facade. Once again, the revised cross-section of this UHPC composite column demonstrated enhanced efficiency to resist blast loading.

This building is designed to be earthquake resistant to 0.98 m/s^2 ground acceleration. However, based on the damage evaluation after the explosion, it may be concluded that the blast loading impact causes the failure with a considerably higher magnitude than those under seismic action. This reveals that the earthquake resistant design is insufficient to withstand blast loading attack with such amount of TNT charge at a small stand-off distance.

4. Conclusions

Based on the theory of the JH-2 model and a subroutine, a series of full 3D numerical models of a 6-story UHPC office building were implemented to interrogate the dynamic behavior of the structure under the explosion of 500 kg TNT equivalent with 8 cases of different blast loading scenario. The following important conclusions are drawn:

1. Under blast loading, the variation of horizontal displacement is non-uniform for the along with the height of the building. This response is different from other impacts like wind and seismic load. The original design assures the structure to withstand the seismic impact. However, it is insufficient to resist an explosion with close distance and large explosive weight.
2. Increasing in the vertical distance and decreasing horizontal distance from the source of explosion leads to increment dramatically in maximum horizontal displacement and damage level of the building. When the distance is close enough, blast loading impact can lead to localized excessive damage, firstly in external columns and joint of the frame

structure, then spreading to other regions and finally triggering the progressive collapse of the whole building. Horizontal displacement is maximum and the 3D frame structure experiences the most severe damage when the blast detonates at the mid-height of the building..

3. Calculation results show that blast can wipe out several columns near the source of the explosion. The revised design of external columns with the UHPC composite structure is demonstrated as a beneficial alternative to improve the overall performance of frame structure and should be selected in blast loading resistance design.

Acknowledgments

Not Applicable

ORCID

Viet-Chinh Mai https://orcid.org/0000-0001-7601-3391
Ngoc-Quang https://orcid.org/0000-0002-8609-3652

References

Abbas A, Adil M, Ahmad N, Ahmad I (2019) Behavior of reinforced concrete sandwiched panels (RCSPs) under blast load. *Engineering Structures* 181:476-490, DOI: 10.1016/j.engstruct. 2018.12.051

Ambrosini D, Luccioni B, Jacinto A, Danesi R (2005) Location and mass of explosive from structural damage. *Engineering Structures* 27(2):167-176, DOI: 10.1016/j.engstruct.2004.09.003

Azmee NM, Shafiq N (2018) Ultra-high performance concrete: From fundamental to applications. *Case Studies in Construction Materials* 9, DOI: 10.1016/j.cscm.2018.e00197

Bao X, Li B (2010) Residual strength of blast damaged reinforced concrete columns. *International Journal of Impact Engineering* 37(3):295-308, DOI: 10.1016/j.ijimpeng.2009.04.003

Buchan PA, Chen JF (2010) Blast protection of buildings using fibre-reinforced polymer (FRP) composites. In: Blast protection of civil infrastructures and vehicles using composites. Woodhead Publishing Limited, Cambridge, UK, 269-297, DOI: 10.1533/9781845698034. 2.269

Cui J, Hao H, Shi Y, Li X, Du K (2017) Experimental study of concrete damage under high hydrostatic pressure. *Cement and Concrete Research* 100:140-152, DOI: 10.1016/j.cemconres.2017.06.005

Dassault Systèmes Simulia Corp. (2016) Abaqus/CAE user's guide. Dassault Systèmes Simulia Corp., Retrieved December 11, 2020, http://130.149.89.49:2080/v6.14/

Department of Defense (2008) Structures to resist the effect of accident explosion. Department of Defense, Retrieved December 11, 2020, http://dod.wbdg.org/

Draganić H, Sigmund V (2012) Blast loading on structures. *Tehnicki Vjesnik* 19(3):643-652

Fu F (2013) Dynamic response and robustness of tall buildings under blast loading. *Journal of Constructional Steel Research* 80:299-307, DOI: 10.1016/j.jcsr.2012.10.001

Hallquist JO, Wainscott B, Schweizerhof K (1995) Improved simulation of thin-sheet metalforming using LS-DyNA3D on parallel computers. *Journal of Materials Processing Technology* 50(1-4):144-157, DOI: 10.1016/0924-0136(94)01376-C

Holmquist TJ, Johnson GR, Cook WH (1993) A computational constitutive model for concrete subjected to large strains, high strain rates and high pressures. *Warhead Mechanisms, Terminal Ballistics* 2:591-600

Ibrahim YE, Nabil M (2019) Assessment of structural response of an existing structure under blast load using finite element analysis. *Alexandria Engineering Journal* 58(4):1327-1338, DOI: 10.1016/ j.aej.2019.11.004

Institute for Economics & Peace (2019) Global terrorism 2019 index: Measuring the impact of terrorism. Institute for Economics & Peace, Retrieved December 11, 2020, https://reliefweb.int/report/world/ global-terrorism-index-2019

Ismail MA, Ibrahim YE, Nabil M, Ismail MM (2017) Response of A 3-D reinforced concrete structure to blast loading. *International Journal of Advanced and Applied Sciences* 4(10):46-53

Jayatilake IN, Dias WPS, Jayasinghe MTR, Thambiratnam DP (2006) Influence of setbacks on the performance of high-rise buildings under blast loadings. Second International Conference on DAPS, Advance in Protective Technology

Johnson GR, Holmquist TJ (1992) A computational constitutive model for brittle materials subjected to large strains, high strain rates and high pressures. In: Meyers M, Murr L, Staudhammer K (eds) Shock wave and high-strain-rate phenomena in materials. CRC Press, Boca Raton, FL, USA, 1075-1081

Khairunnisa M, Zahid MZAM, Rafiza AR, Nurfitriah I, Zainol NZ, Manaf MBHA, Ahmad MM, Aishah SNMN, Noh NN, Johari MZ, Zaidi ASSM (2018) Ultra high performance fibre reinforced concrete mixture proportion - A review. *AIP Conference Proceedings* 2030(1), DOI: 10.1063/1.5066938

Kong XQ, Zhao Q, Qu YD, Zhang WJ (2018) Blast response of cracked reinforced concrete slabs repaired with CFRP composite patch. *KSCE Journal of Civil Engineering* 22(4):1214-1224, DOI: 10.1007/ s12205-017-1054-3

Livermore Software Technology Corporation (2007) LS-DYNA keyword user's manual. Livermore Software Technology Corporation, Livermore, CA, USA

Mai V-C, Vu N-Q, Pham H, Nguyen V-T (2020) Ultra-high performance fiber reinforced concrete panel subjected to severe blast loading. *Defence Science Journal* 70(6):603-611, DOI: 10.14429/dsj.70.15835

Mao L, Barnett S, Begg D, Schleyer G, Wight G (2014) Numerical simulation of ultra high performance fibre reinforced concrete panel subjected to blast loading. *International Journal of Impact Engineering* 64:91-100, DOI: 10.1016/j.ijimpeng.2013.10.003

Ngo T, Mendis P, Gupta A, Ramsay J (2007) Blast loading and blast effects on structures - An overview. *Electronic Journal of Structural Engineering* 7:76-91

Ousalem H, Takatsu H, Ishikawa Y, Kimura H (2009) Use of high-strength bars for the seismic performance of high-strength concrete columns. *Journal of Advanced Concrete Technology* 7(1):123-134, DOI: 10.3151/jact.7.123

Shin J, Lee K (2018) Blast performance evaluation of structural components under very near explosion. *KSCE Journal of Civil Engineering* 22(2):777-784, DOI: 10.1007/s12205-017-1889-7

Shinde P, Shinde S, Kulkarni M (2019) Comparitive study of steel fibre reinforced concrete panels and ferrocement panels under blast loading by fem analysis. *International Journal of Scientific and Technology Research* 8(8):1436-1441

Smarzewski P (2019) Study of toughness and macro/micro-crack development of fibre-reinforced ultra-high performance concrete after exposure to elevated temperature. *Materials* 12(8), DOI:

10.3390/ma12081210

Tayeh BA, Aadi AS, Hilal NN, Bakar BHA, Al-Tayeb MM, Mansour WN (2019) Properties of ultra-high-performance fiber-reinforced concrete (UHPFRC) - A review paper. *AIP Conference Proceedings* 2157(1), DOI: 10.1063/1.5126575

Thilakarathna HMI, Thambiratnam DP, Dhanasekar M, Perera N (2010) Numerical simulation of axially loaded concrete columns under transverse impact and vulnerability assessment. *International Journal of Impact Engineering* 37(11):1100-1112, DOI: 10.1016/j.ijimpeng.2010.06.003

Vietnamese Ministry of Construction (2011) TCVN 2737:1995 - Load and effects - Design standard. Construction Publisher, Hanoi, Vietnam

Vietnamese Ministry of Construction (2013) TCVN 9386:2012 - Design of structures for earthquake resistance. Construction Publisher, Hanoi, Vietnam

Wang D, Shi C, Wu Z, Xiao J, Huang Z, Fang Z (2015) A review on ultra high performance concrete: Part II. Hydration, microstructure and properties. *Construction and Building Materials* 96:368-377, DOI: 10.1016/j.conbuildmat.2015.08.095

Wang Z, Wang J, Liu T, Zhang F (2016) Modeling seismic performance of high-strength steel-ultra-high-performance concrete piers with modified Kent-Park model using fiber elements. *Advances in Mechanical Engineering* 8(2):1-14, DOI: 10.1177/1687814016633411

Weerheijm J, Van Doormaal A, Villa JM (2008) Concrete structures under blast loading dynamic response, damage, and residual strength. In: Pasman HJ, Kirillov IA (eds) Resilience of cities to terrorist and other threats. Springer, Berlin, Germany, 217-238, DOI: 10.1007/978-1-4020-8489-8_11

Weerheijm J, Mediavilla J, Van Doormaal JCAM (2009) Explosive loading of multi storey RC buildings: Dynamic response and progressive collapse. *Structural Engineering and Mechanics* 32(2):193-212, DOI: 10.12989/sem.2009.32.2.193

Yandzio E GM (1999) Protection of buildings against explosions. Steel Construction Institute, Ascot, UK

Yoo DY, Banthia N (2017) Mechanical and structural behaviors of ultra-high-performance fiber-reinforced concrete subjected to impact and blast. *Construction and Building Materials* 149:416-431, DOI: 10.1016/j.conbuildmat.2017.05.136